Decreased Methylenetetrahydrofolate Reductase Activity Leads to Increased Sensitivity to *para*-Aminosalicylic Acid in *Mycobacterium tuberculosis*

Ji-fang Yu,[a,b] Jin-tian Xu,[a,b] Shan-shan Yang,[a] Mei-na Gao,[c] Hao-rui Si,[a,b] Dong-yan Xiong,[a,b] Jing Gu,[a] Zhi-long Wu,[d] Jie Zhou,[d] Jiao-yu Deng[a,e]

aKey Laboratory of Special Pathogens and Biosafety, Wuhan Institute of Virology, Center for Biosafety Mega-Science, Chinese Academy of Sciences, Wuhan, People's Republic of China

bUniversity of Chinese Academy of Sciences, Beijing, People's Republic of China

cSchool of Chinese Materia Medica, Nanjing University of Chinese Medicine, Nanjing, People's Republic of China

dFoshan Fourth People's Hospital, Foshan, People's Republic of China

eGuangdong Province Key Laboratory of TB Systems Biology and Translational Medicine, Foshan Institude of Industrial Technology, Chinese Academic of Sciences, Foshan, People's Republic of China

Ji-fang Yu and Jin-tian Xu contributed equally to this work and share first authorship, and the order was determined alphabetically.

ABSTRACT Tuberculosis (TB), caused by *Mycobacterium tuberculosis*, is one of the most fatal diseases in the world. Methylenetetrahydrofolate reductase (MTHFR) catalyzes the production of 5-methyltetrahydrofolate (5-CH$_3$-THF), which is required for the *de novo* biosynthesis of methionine in bacteria. Here, we identified Rv2172c as an MTHFR in *M. tuberculosis* through *in vitro* and *in vivo* analyses and determined that the protein is essential for the *in vitro* growth of the bacterium. Subsequently, we constructed *rv2172c* R159N and L214A mutants in *M. tuberculosis* and found that these mutants were more sensitive to the antifolates *para*-aminosalicylic acid (PAS) and sulfamethoxazole (SMX). Combining biochemical and genetic methods, we found that *rv2172c* R159N or L214A mutation impaired methionine production, leading to increased susceptibility of *M. tuberculosis* to PAS, which was largely restored by adding exogenous methionine. Moreover, overexpression of *rv2172c* in *M. tuberculosis* could increase methionine production and lead to PAS resistance. This research is the first to identify an MTHFR in *M. tuberculosis* and reveals that the activity of this enzyme is associated with susceptibility to antifolates. These findings have particular value for antitubercular drug design for the treatment of drug-resistant TB.

KEYWORDS *Mycobacterium tuberculosis*, methylenetetrahydrofolate reductase, Rv2172c, *para*-aminosalicylic acid, methionine

Tuberculosis (TB), caused by *Mycobacterium tuberculosis*, is still one of the most lethal human diseases. *M. tuberculosis* is responsible for 10.0 million new cases of active TB and 1.5 million deaths annually (1). Since rifampicin was first used in a clinic in the 1968 (2), no new first-line antitubercular drugs have been identified over the past 50 years. By the 1990s, the emergence and spread of multidrug-resistant tuberculosis (MDR-TB) and extensively drug resistant tuberculosis (XDR-TB) has made the prevention and treatment of TB more challenging (3, 4). In order to fundamentally solve the problem of TB drug resistance, identifying new targets for drug design is essential. Additionally, it is equally important to further study the basic biology of *M. tuberculosis*, including the molecular mechanisms of *M. tuberculosis* sensitivity, resistance, and tolerance to existing antitubercular drugs.

Para-aminosalicylic acid (PAS) was the second antitubercular drug identified for clinical use, after streptomycin (5–7). PAS acts as a prodrug that activated by dihydropteroate
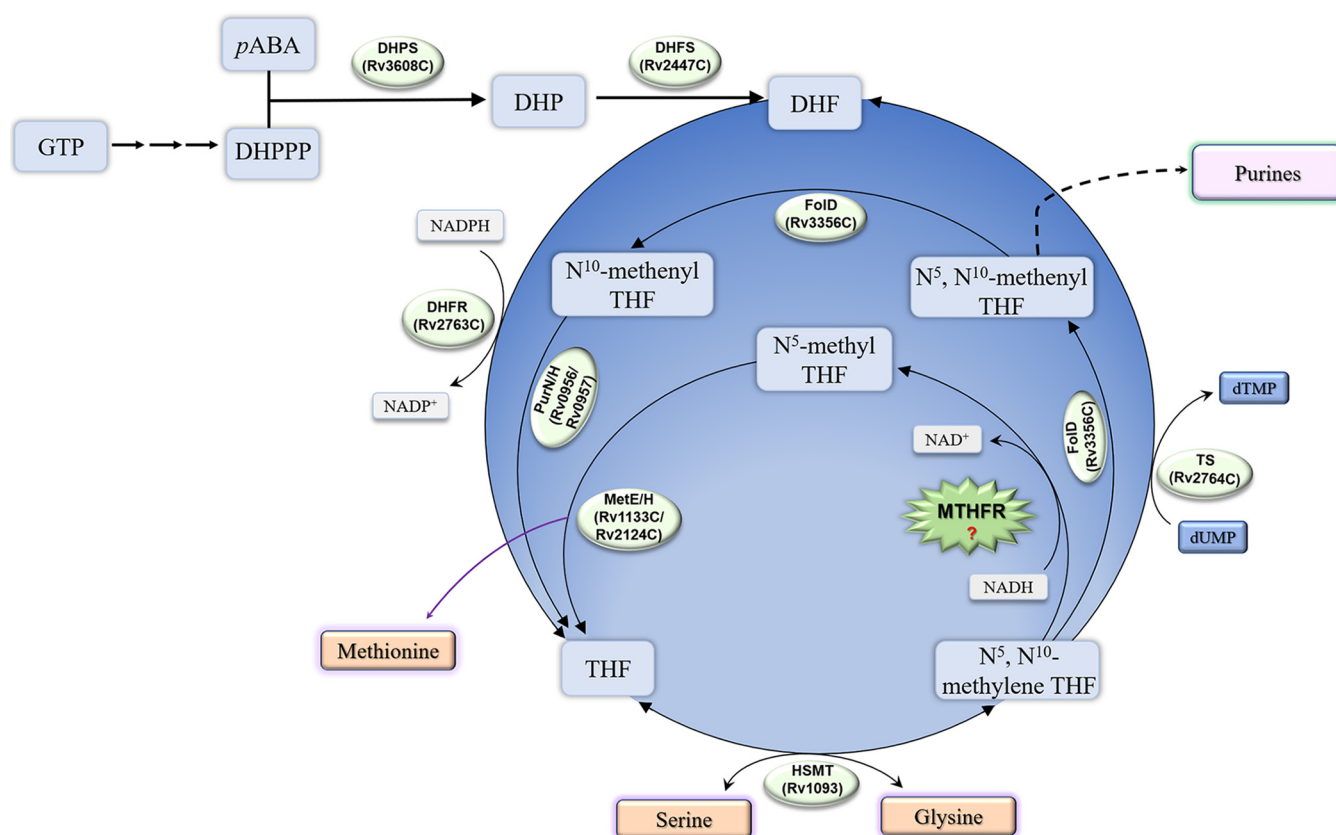
synthase (DHPS) and dihydrofolate synthase (DHFS) before finally targeting dihydrofolate synthase (DHFR) in the folate biosynthesis pathway (6, 7). Sulfonamides were also the earliest identified antibacterial drugs (8). These compounds target the DHPS, which catalyzes the addition of dihydropterin diphosphate to p-aminobenzoic acid (pABA) (8–10). As structural analogs of pABA, sulfonamides compete with pABA, leading to the waste of dihydropterin diphosphate and the blockage of dihydropteroate biosynthesis (8–10). Sulfamethoxazole (SMX; a kind of sulfonamide) and PAS were both important components in early TB chemotherapies, especially PAS (5). In later years, the introduction of more potent and less toxic antitubercular drugs regimens diminished their usage. With the emergence of MDR-TB and XDR-TB, PAS has returned to clinical application (11, 12). Moreover, SMX has been receiving increasing attention as a treatment for drug-resistant TB (13–15). PAS and SMX are both antifolates that inhibit *de novo* folate biosynthesis in bacteria (5, 8). Folate provides an important one-carbon for bacteria and is crucial for the *de novo* synthesis of methionine, purines, and deoxythymidine monophosphate (dTMP) (16). In addition, methionine is a potent antagonist of PAS (17, 18).

As the lynchpin of folate downstream metabolism, methylenetetrahydrofolate reductase (MTHFR) catalyzes the NAD(P)H-dependent reduction of 5,10-methylenetetrahydrofolate (5,10-CH_2-THF) to 5-methyltetrahydrofolate (5-CH_3-THF) (19). This reaction is the sole source of bacterial methyltetrahydrofolate (20), which provides one-carbon units for the synthesis of methionine and maintains the recycling and homeostasis of tetrahydrofolate. MTHFR is encoded by the *metF* gene in *Escherichia coli*. Previous research has shown that *E. coli* MTHFR has NADH-dependent reductase activity and uses either flavin adenine dinucleotide (FAD) or flavin mononucleotide (FMN) as a source of reducing equivalents for the reduction of 5,10-CH_2-THF to 5-CH_3-THF (19, 21, 22). MTHFR's catalytic domain contains an $\alpha_8\beta_8$ barrel (23). Mutation of Phe223 decreases both substrate and NADH binding (23, 24), while Asp120 mutation reduces MTHFR's affinity for 5-CH_3-THF (25), and Glu28 (proton donor or acceptor) mutation abolishes the enzymatic activity of MTHFR (25, 26). A nucleotide phosphate-binding region (NPBR), located from amino acids 165 to 172, was also shown to be important for enzyme activity due to FAD binding (23). Although the properties and crystal structure of *E. coli* MTHFR have been extensively explored (23–27), MTHFR in *M. tuberculosis* has not been uniquely identified or annotated. A previous review article revealed the important clue that Rv2172c might be an atypical MetF homologue, because its predicted structure significantly matched the crystal structure of MetF from *Thermus thermophilus* (28). Unfortunately, there were no further experimental data following this observation. Here, using *E. coli* W3110 and *M. tuberculosis* H37Ra as bacterial models, we carried out a series of experiments *in vitro* and *in vivo* to characterize whether Rv2172c was the MTHFR in *M. tuberculosis*. Additionally, we aimed to reveal the relationship between the activity of Rv2172c and the sensitivity of *M. tuberculosis* to antifolate PAS.

RESULTS

The predicted three-dimensional structure of Rv2172c has relatively high similarity to the structure of *E. coli* MTHFR. MTHFR is a crucial enzyme in folate downstream metabolism, but it remains unidentified in *M. tuberculosis* (Fig. 1). We aligned the primary sequence of Rv2172c with MTHFR homologues from several *Enterobacter* species. The results showed that the enzymes from *Enterobacter* had significant primary sequence homology, while Rv2172c showed very low similarity to these (Fig. 2A). Considering the differences between these two genera in terms of GC content, protein translation, and direction of bacteria evolution, we predicted the secondary structure of Rv2172c using Phyre 2 as previously reported (29). We found that the high-confidence template was a mutated *E. coli* MTHFR Ala177Val (Fig. 2B; see also Fig. S1A in the supplemental material). In addition, most matched templates all had methylenetetrahydrofolate reductase activity (Fig. S1B). Next, structural modeling of Rv2172c revealed a higher similarity with MTHFR from *E. coli* (PDB entry 1ZP3) than with primary sequence homology (Fig. 3).
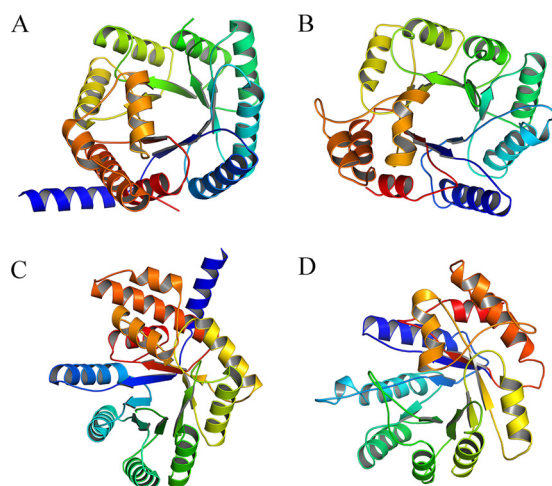
FIG 1 MTHFR remains unknown in *M. tuberculosis*. MTHFR, 5,10-methylenetetrahydrofolate reductase; DHPS, dihydropteroate synthase; DHFS, dihydrofolate synthase; DHFR, dihydrofolate reductase; TS, thymidylate synthase; MetE, cobalamin-independent homocysteine transmethylase; MetH, cobalamin-dependent methionine synthase; FolD, bifunctional 5,10-methylenetetrahydrofolate dehydrogenase/cyclohydrolase; PurH, bifunctional AICAR formyltransferase/IMP cyclohydrolase; PurN, phosphoribosylglycinamide formyltransferase; HSMT, serine hydroxymethyltransferase.

Rv2172c complemented the growth defect of the *E. coli* Δ*metF* strain. As shown in Fig. 4A, MTHFR converts 5,10-CH$_2$-THF to 5-CH$_3$-THF, and then methionine synthase (MetH/E) catalyzes the transfer of a methyl group from 5-CH$_3$-THF to homocysteine to form methionine (19, 30). This MTHFR activity is thus crucial for methionine biosynthesis in bacteria, and deleting MTHFR-encoding genes leads to a methionine auxotroph phenotype. To test our putative *M. tuberculosis* MTHFR, we knocked out the MTHFR-coding gene *metF* in *E. coli*, which resulted a methionine auxotroph phenotype, as expected (Fig. 4B and C). The growth defect caused by *metF* deletion could be rescued by adding exogenous methionine *in vitro*, and the bacterial growth was methionine dose dependent (Fig. 4C). To explore the physiological role of *rv2172c* in *M. tuberculosis* and verify whether Rv2172c has MTHFR activity *in vivo*, we tested the ability of Rv2172c to rescue the methionine auxotroph phenotype of the *E. coli* W3110 Δ*metF* strain. As shown in Fig. 4B and D, transformation with pCA24N::*rv2172c* or pCA24N::*metF* in the *E. coli* W3110 Δ*metF* strain both conferred growth in cultures on E medium without exogenous methionine addition.

Rv2172c catalyzes 5,10-methylenetetrahydrofolate to produce 5-methyltetrahydrofolate in the presence of NADH. Subsequently, we designed five reaction systems to assess the reductase activity of purified Rv2172c *in vitro* (see Fig. S2, inset table). MTHFR could utilize 5,10-CH$_2$-THF (Fig. S2A) as a substrate to produce 5-CH$_3$-THF (Fig. S2B). To identify the product formed in these reaction mixtures, high-performance liquid chromatography–mass spectrometry (HPLC-MS) analysis was performed. The base peak chromatogram from reaction 2 (Fig. 5A, II) showed the emergence of a new peak (at ~13 min, red frame), which was identified as the product 5-CH$_3$-THF based on the MS peak at 460.22 *m/z* (Fig. 5C). The substrate 5,10-CH$_2$-THF (*m/z* = 458.27) in this

A

B

FIG 2 The homology of Rv2172c from *M. tuberculosis* with MTHFR in *E. coli*. (A) Rv2172c and several *Enterobacter* MTHFR primary sequence alignment. (B) Prediction of Rv2172c protein secondary structure using Phyre 2. Each row from the top to the bottom is Rv2172c predicted secondary structure, Rv2172c primary sequence, template *E. coli* MTHFR primary sequence, template *E. coli* MTHFR known secondary structure, and template *E. coli* MTHFR predicted secondary structure (as the control to test the confidence of prediction). Identical residues in the alignment are highlighted with a gray background. Residues marked by blue boxes are the residues of *E. coli* MTHFR interacting with FAD, as claimed in previous studies (23, 24). Residues marked by red boxes are catalytic residues from the Catalytic Site Atlas (CSA).

FIG 3 The predicted three-dimensional (3D) structure of Rv2172c compared with the known structure of *E. coli* MetF. Rv2172c was modeled based on the best-matched template from *Thermus thermophilus* MTHFR (PDB entry 3APT). (A) Front view of MetF, (B) front view of Rv2172c, (C) side view of MetF, and (D) side view of Rv2172c.

reaction in the base peak chromatogram (at ~16.8 min, blue frame) was also confirmed by MS analysis (Fig. 5B). When Rv2172c was absent, this reaction did not proceed (Fig. 5A, I). This protein had an NADH-dependent, but FAD-nondependent, reductase activity (Fig. 5A, III and IV). This was different from MetF of *E. coli*, but consistent with the MTHFR in *Mycobacterium smegmatis* (31). Additionally, a few FAD-interacting amino acids from MetF (23, 24) were found in similar locations in Rv2172c (Fig. 2B).

The Rv2172c L214A and Rv2172c R159N mutants in *M. tuberculosis* showed reduced methionine production and growth defects. We next tried to knock out *rv2172c* in *M. tuberculosis* by supplementing exogenous methionine into the growth medium but failed (data not shown). The original copy of the *rv2172c* gene on the *M. tuberculosis* chromosome could be deleted only in the presence of another copy of *rv2172c* introduced using a recombinant plasmid. Thus, we changed our tactic for constructing mutant strains that harbored point mutations in the *rv2172c* gene (Table S1). To achieve this, we first introduced the mutant genes into *M. tuberculosis* by using the recombinant plasmid pMV361 and then deleted the original copy of the *rv2172c* gene in the chromosome. The corresponding "Rv2172c (WT)" strain was also constructed through the same procedure; in this case, an intact *rv2172c* gene was introduced into the bacterium by using the same plasmid.

To select suitable mutation sites, a modeled three-dimensional (3D) structure of Rv2172c (pink) was superimposed on the *E. coli* MTHFR structure (PDB entry 1ZP3) (blue). As shown in Fig. 6A, the known key catalytic residues (Glu28, Asp120, and Phe223) in *E. coli* MTHFR and their corresponding sites in Rv2172c were mapped. The center of the region from amino acids 165 to 172 in *E. coli* MTHFR, Asn168 (Arg159 in Rv2712c), was also utilized. We tried to mutate these four amino acid residues in *rv2712c*, but successfully constructed only two mutants (*rv2172c* L214A and R159N) (Fig. 6B).

We speculated that Arg159 or Leu214 were important for the MTHFR activity of Rv2172c and that R159N or L214A mutation might disturb methionine synthesis in *M. tuberculosis*. To detect the methionine content in these mutants, ultraperformance liquid chromatography-tandem mass spectrometry (UPLC-MS/MS) analysis was performed. As shown in Fig. 7A, the methionine content of Rv2172c R159N or L214A was significantly lower than that of the "Rv2172c (WT)" strain.

Without adding exogenous methionine, the *E. coli metF* knockout strain showed no growth on minimal medium. The Rv2172c R159N or L214A mutants also showed some degree of growth defect compared to the "Rv2172c (WT)" strain (Fig. 7B and C).
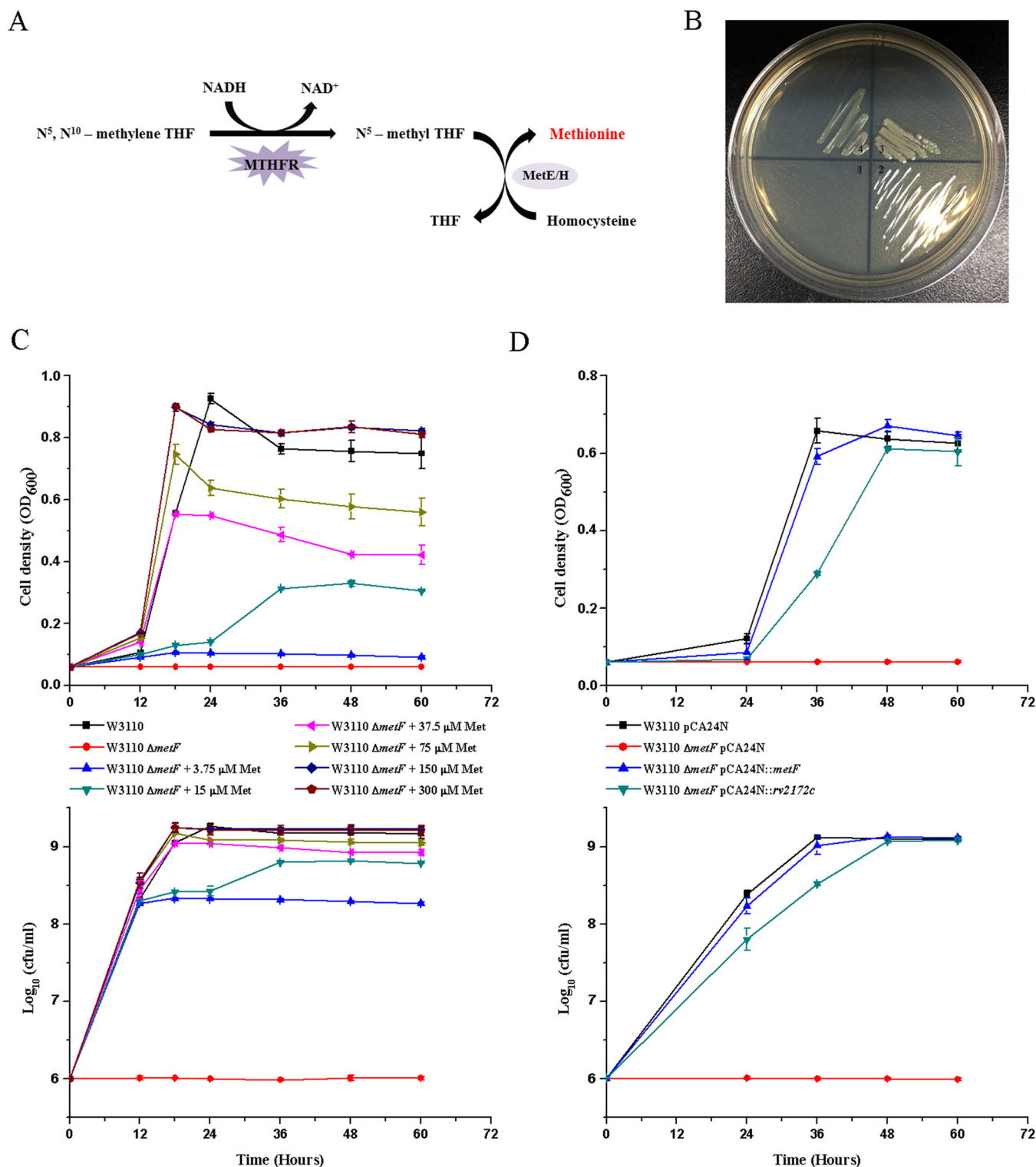
FIG 4 The MTHFR activity of Rv2172c *in vivo*. (A) MTHFR reaction downstream of the methionine synthesis pathway. (B) *E. coli* W3110 Δ*metF* strains harboring (1) no vector, (2) empty pCA24N vector, (3) pCA24N::*metF*, and (4) pCA24N::*rv2172c* were inoculated on solid minimal medium. (C) *E. coli* W3110 Δ*metF* was cultured on minimal medium containing different concentrations of methionine (Met). *E. coli* W3110 was used as a control. Optical density at 600 nm (OD$_{600}$) (upper) and log$_{10}$ CFU (lower) were measured at appropriate times. (D) *E. coli* W3110 Δ*metF* strains harboring empty pCA24N vector, pCA24N::*metF*, or pCA24N::*rv2172c* were cultured on minimal medium. *E. coli* W3110 pCA24N was the control background. OD$_{600}$ (up) and log$_{10}$ CFU (down) were measured at appropriate times. The experiments were performed using three biological replicates. The standard deviations (SDs) are indicated by the error bars, and the data are reported as mean ± SD.
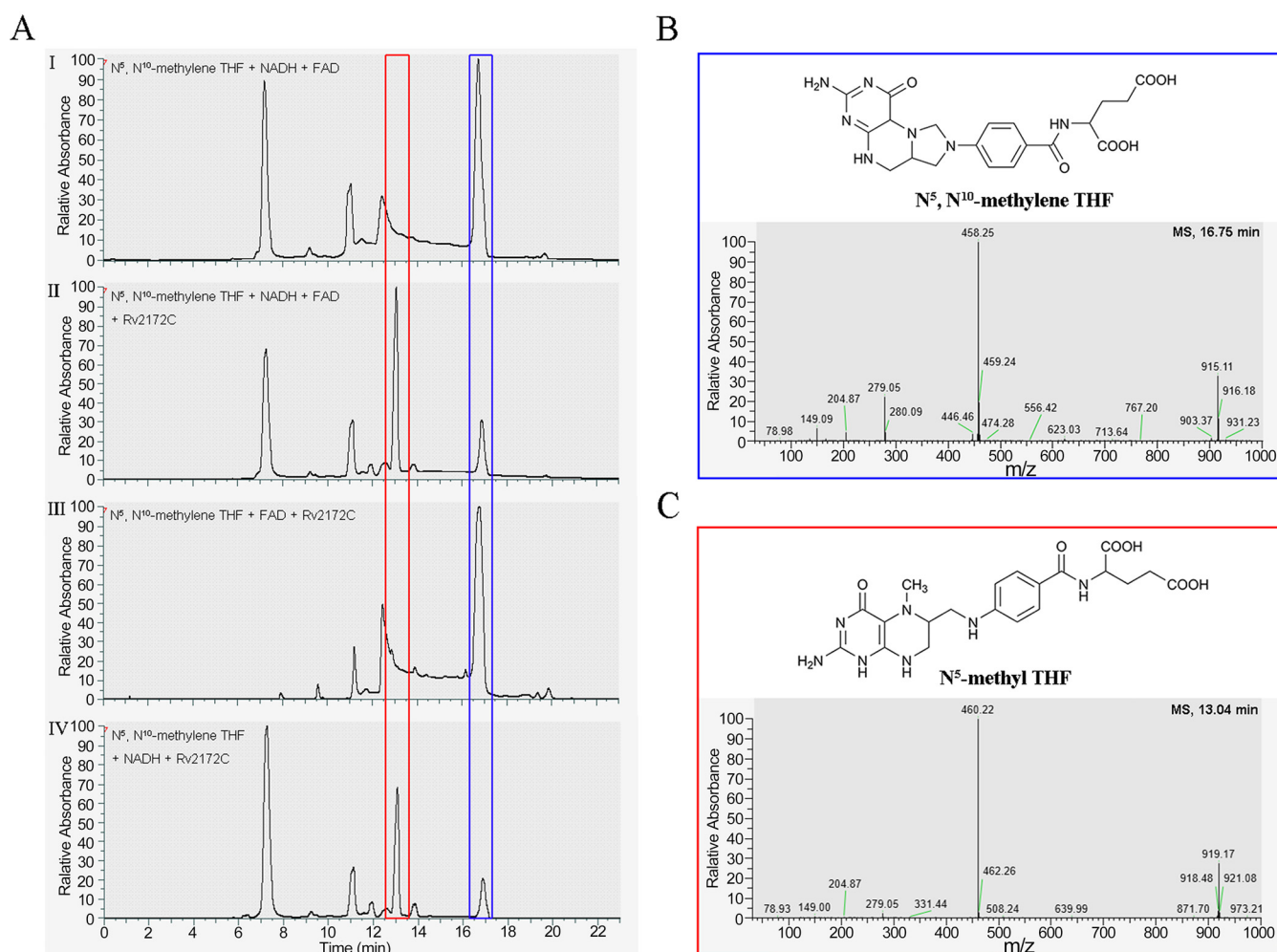
FIG 5 The reductase activity of Rv2172c by high-performance liquid chromatography–mass spectrometry (HPLC-MS). (A) HPLC analysis from different reaction systems containing (I) 5,10-CH$_2$-THF, NADH, and FAD, (II) 5,10-CH$_2$-THF, NADH, FAD, and Rv2172c; (III) 5,10-CH$_2$-THF, FAD, and Rv2172c; and (IV) 5,10-CH$_2$-THF, NADH, and Rv2172c. (B) The substrate in reaction system 2, 5,10-CH$_2$-THF, was identified based on an MS peak at 458.25 *m/z*. (C) The product in reaction system 2, 5-CH$_3$-THF, was identified based on an MS peak at 460.22 *m/z*.

Rv2172c L214A and Rv2172c R159N mutants showed increased susceptibility to PAS and SMX. Previous studies have shown that methionine is a potent antagonist of PAS (17, 18). Since the mutations L214A and R159N led to decreased methionine production in *M. tuberculosis*, we speculated that these two mutations might affect susceptibility to PAS. SMX and PAS are both commonly used antifolates, and MTHFR is a crucial enzyme in folate metabolism. Therefore, the susceptibilities of these two mutants to PAS and SMX were determined using a MIC assay. As shown in Table 1, the MICs of PAS and SMX in the Rv2172c L214A mutant were 20-fold and 32-fold lower, respectively, than that of the "Rv2172c (WT)" strain. The MICs of PAS and SMX in the Rv2172c R159N mutant were 20-fold and 4-fold lower, respectively, than that of the "Rv2172c (WT)" strain. In the "Rv2172c (WT)" strain (H37Ra Δ*rv2172c* pMV361::*rv217c*), the chromosomal copy of *rv2172c* was replaced by an intact *rv2172c* under the control of the Hsp60 promoter, resulting in overexpression of the gene and decreased susceptibility to PAS compared to that of the H37Ra strain.

Exogenous methionine rescues the growth defect of Rv2172c L214A and Rv2172c R159N, reversing their increased sensitivities to PAS. In order to determine whether the growth defect of these two mutants was caused by reduced methionine production *in vivo*, we added two concentrations of methionine to our growth medium and compared the growth curves of Rv2172c R159N and Rv2172c L214A with
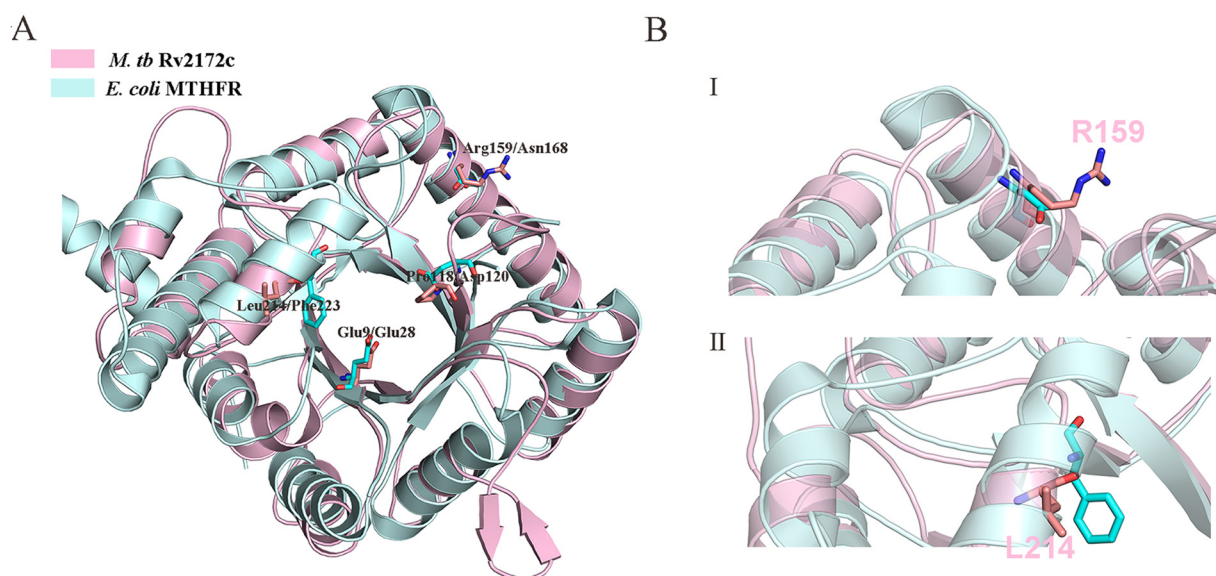
FIG 6 Comparison between a modeled structure of Rv2172c and the known structure of *E. coli* MTHFR. Rv2172c was modeled based on *E. coli* MetF (PDB entry 1ZP3). (A) Superimposition of these two structures highlights the high structural similarity at the level of the overall fold. Close-up view of the active site predicted from previous studies, including catalytic residues such as Glu9/Glu28, Pro118/Asp120, Arg159/Asn168, and Leu214/Phe223 (*M. tuberculosis* Rv2172c/*E. coli* MetF). (B) Representation of the catalytic residues (I) R159 and (II) L214.

that of the "Rv2172c (WT)" strain. As shown in Fig. 7B and C, the growth defect of these mutants could be largely restored by adding exogenous methionine. Moreover, 150 μM or 300 μM methionine worked similarly in this context. This indicated that 150 μM methionine might be sufficient to support the *in vitro* growth of these two mutants. In contrast, 150 μM methionine could completely reverse the bactericidal effect of PAS (Fig. 8A). Thus, the MICs of PAS in these two Rv2172c mutants and the "Rv2172c (WT)" strain in the presence of 150 μM methionine were tested. As shown in Table 2, in the presence of methionine, both of these two mutants became highly resistant to PAS.

Overexpressing *rv2172c* in *M. tuberculosis* increased the production of methionine but decreased *M. tuberculosis* sensitivity to PAS. To further explore how mutations in *rv2172c* changed the sensitivity to PAS in *M. tuberculosis*, *rv2172c* and other methionine synthase coding genes (*metE* and *metH*) were overexpressed in *M. tuberculosis*. The results showed that overexpressing all of these genes led to PAS resistance in *M. tuberculosis* (Table 3). Correspondingly, we observed an obvious increase in methionine production in the *rv2172c* overexpression strain compared to the wild-type (WT) strain (Fig. 8B).

Mutation analysis of *rv2172c* in *M. tuberculosis*. We analyzed a library of 6,568 *M. tuberculosis* genomes from isolates classified as clinical (*n* = 6,310) and environmental or other (*n* = 258) from the National Center for Biotechnology Information (NCBI) database (Table S2). We found that the summed rate of nonsynonymous, indel, and nonsense single-nucleotide polymorphisms (SNPs) in *rv2172c* was very low (~1%) in both the clinical and environmental isolates, and the major mutations identified in the environment isolates were synonymous mutations (Table 4). This indicated that the primary sequence of Rv2172c was relatively conserved.

To further investigate the potential clinical relevance of *rv2172c* and PAS susceptibility, mutations of *rv2172c* and 3 other genes related to PAS resistance, *folC* (32, 33), *thyA* (32, 34, 35), and *ribD* (7, 32), were characterized by analyzing the whole-genome sequence of 52 PAS-resistant clinical isolates (Table S3). As shown in Table 5, the mutation rates of *folC* (40.38%), *thyA* (34.62%), and *ribD* (3.85%) were all within a normal fluctuation compared to the previous studies (32, 34). To our surprise, the mutation rate of *rv2172c* in the 52 PAS-resistant isolates was 9.62%, even higher than that of *ribD*. Two specific mutations were identified, T120P (5.77%) and M172V (3.85%). Thus,
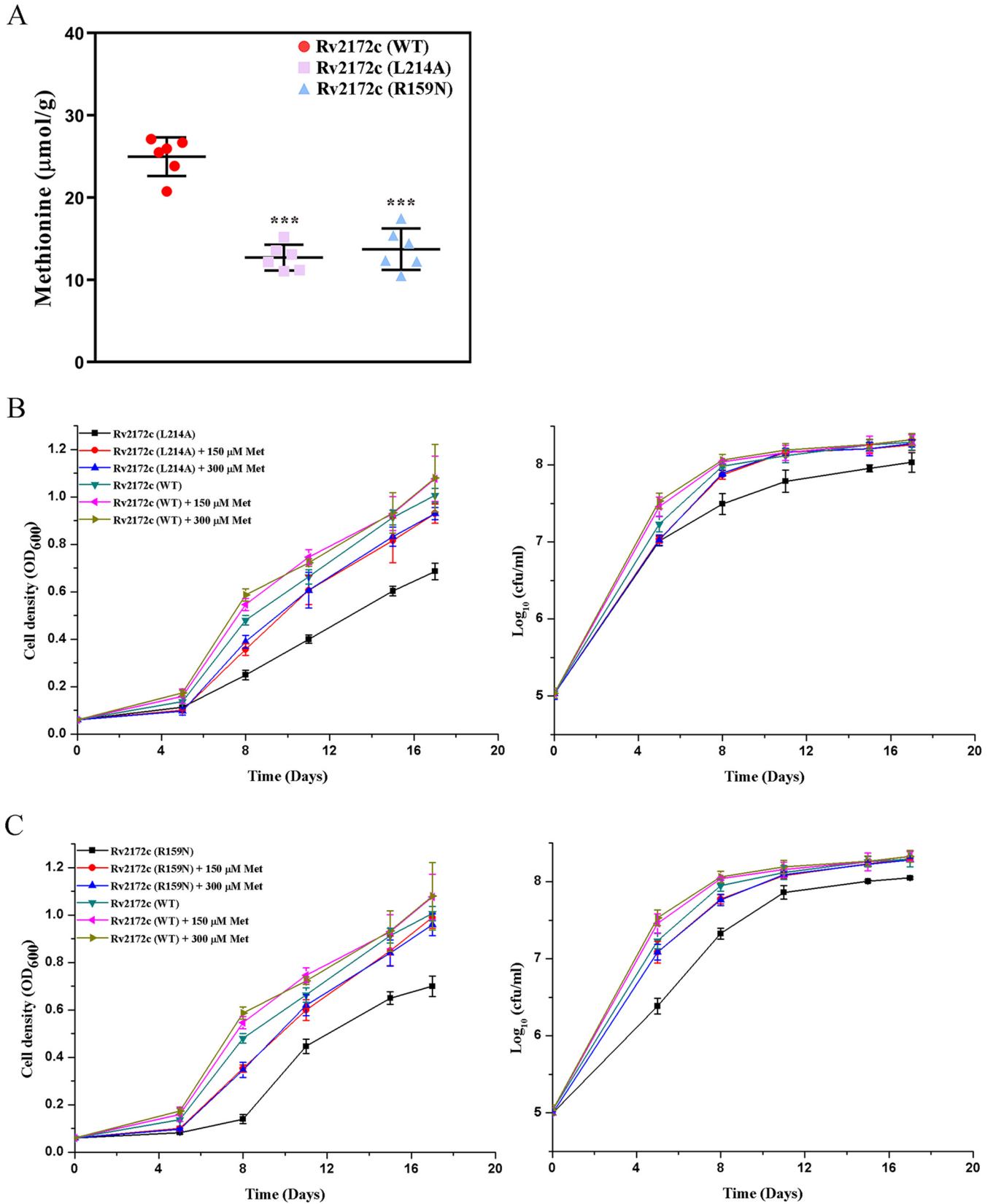
FIG 7 Assessment of the constitutive synthesis of methionine in *rv2172c* mutants. (A) The constitutive synthesis of methionine in *rv2172c* mutant cells was measured by ultraperformance liquid chromatography-tandem mass spectrometry (UPLC-MS/MS). Cell-associated methionine was extracted from Rv2172c (WT), Rv2172c (L214A), and Rv2172c (R159N) strains and quantified as described in Materials and Methods. The experiments were performed using six

(Continued on next page)

TABLE 1 Replacement of Rv2172c with Rv2172c L214A and R159N confers sensitivity to the antifolates PAS and SMX in *M. tuberculosis* H37Ra

	MIC (μg $\cdot$ mL^{-1}) for:	
Strain[a]	PAS	SMX
Rv2172c (WT)	0.2	100
Rv2172c (L214A)	0.01	3.125
Rv2172c (R159N)	0.01	25

[a]Rv2172c (WT), H37Ra Δ*rv2172c* pMV361::*rv2172c*. Rv2172c (L214A), H37Ra Δ*rv2172c* pMV361::*rv2172c* (L214A). Rv2172c (R159N), H37Ra Δ*rv2172c* pMV361::*rv2172c* (R159N).

we further analyzed the mutation of *rv2172c* in 66 PAS-sensitive clinical isolates presented in previous work (Table S3). The mutation of *rv2172c* was found in one of the 66 PAS-sensitive isolates. The rate of this mutation, M172V (1.51%; 1/66), was lower in the PAS-sensitive isolates than that in the PAS-resistant isolates. In addition, the T120P mutation was not found in the 66 PAS-sensitive isolates.

DISCUSSION

Although it is well known that 5-CH$_3$-THF is an essential cofactor for bacterial methionine synthase, the enzyme catalyzing the production of 5-CH$_3$-THF in *M. tuberculosis* has not yet been identified or characterized. Here, we show that *rv2172c* encodes an MTHFR in *M. tuberculosis*. Previously, Umesh et al. showed that there were two copies of MTHFR in *M. smegmatis*, MSMEG_6596 and MSMEG_6649 (31). Deletion of the major MTHFR encoding gene (*mseg_6596*) caused a partial methionine auxotroph in *M. smegmatis*, indicating they might be jointly essential for methionine biosynthesis. In *M. tuberculosis*, however, Rv2172c seems to be the only copy of an MTHFR, since *rv2172c* is essential for the *in vitro* growth of this bacterium. Although the MTHFR encoding gene *metF* was also shown to be essential for the *in vitro* growth of *E. coli* on minimum medium, an *metF* deletion mutant was successfully constructed by supplementing the growth medium with exogenous methionine. However, the original copy of *rv2172c* on the *M. tuberculosis* chromosome could be deleted only in the presence of another copy of *rv2172c*, in this case introduced by a recombinant plasmid. Otherwise, not a single transductant was obtained on 7H10 plates supplemented with 10% oleic acid-albumin-dextrose-catalase (OADC) and sufficient methionine. All of these data suggest that either Rv2172c has another yet unknown important function in addition to being an MTHFR, or that 5-CH$_3$-THF participates in another essential physiological process in *M. tuberculosis* in addition to methionine biosynthesis, which merits further investigation.

PAS and SMX are two commonly used antifolates, and both are effective against *M. tuberculosis* (11–15). In the 1950s, it was found that methionine could antagonize the growth inhibition effect of PAS on *M. tuberculosis* (17, 18). Recently, Howe et al. showed that this antagonism could be abolished by disrupting *para*-aminobenzoic acid biosynthesis (36). Besides, the susceptibility to sulfonamides in *M. tuberculosis* was also shown to be associated with methionine, since deleting *metH* led to increased sensitivity to sulfonamides (37). These findings indicated that disturbing methionine synthesis might affect susceptibility to PAS and SMX in *M. tuberculosis*. As is well known, the pharmacodynamics of PAS and SMX are quite different. Here, we focused more on PAS, which is presently used as a second-line antituberculosis drug. Theoretically, there are multiple ways to disrupt methionine biosynthesis. Here, we show that decreasing methylenetetrahydrofolate reductase activity leads to decreased production of methionine in *M. tuberculosis* and hence makes this bacterium more sensitive to PAS. Methionine is an essential amino acid for humans, who have to

FIG 7 Legend (Continued)
biological replicates. *P* values were calculated using *t* tests. ***, $P < 0.001$. (B) Growth curves for Rv2172c (WT) and Rv2172c (L214A) in 7H9 (with OADC), in the presence of 150 μM or 300 μM methionine (Met). (C) Growth curves of Rv2172c (WT) and Rv2172c (R159N) in 7H9 (with OADC) with 150 μM or 300 μM methionine (Met). Rv2172c (WT), H37Ra Δ*rv2172c* pMV361::*rv2172c*; Rv2172c (L214A), H37Ra Δ*rv2172c* pMV361::*rv2172c* (L214A); Rv2172c (R159N), and H37Ra Δ*rv2172c* pMV361::*rv2172c* (R159N). OD$_{600}$ (left) and log$_{10}$ CFU (right) were measured at appropriate times. No addition of methionine was used as a control condition. Data represent the mean $\pm$ SD.

A

B
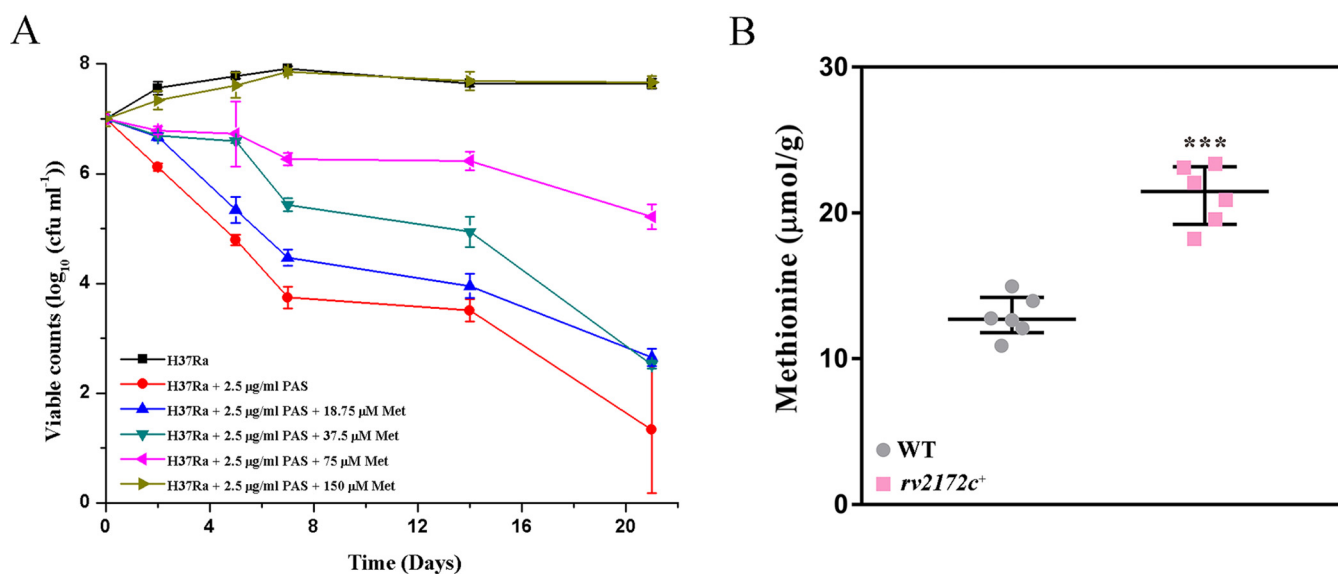
FIG 8 Methionine antagonize PAS and the quantitative detection of methionine by UPLC-MS/MS in *rv2172c* overexpression strains. (A) H37Ra was cultured in 7H9 broth (with OADC), containing 2.5 μg/mL PAS and different concentrations of methionine (Met). No PAS addition was used as a control. Experiments were performed using three biological replicates. Data represent the mean $\pm$ SD. (B) The synthesis of methionine in the *rv2172c* overexpression strains was detected via UPLC-MS/MS. Cell-associated methionine was extracted from WT (H37Ra pMV261) and *rv2172c*[+] (H37Ra pMV261::*rv2172c*) strains and quantified as described in Materials and Methods. The experiments were performed using six biological replicates. *P* values were calculated using *t* tests. ***, $P < 0.001$.

ingest it from their diet. Bacteria, including *M. tuberculosis*, have a *de novo* synthesis pathway for methionine, and disrupting this usually causes a methionine auxotroph phenotype. Moreover, Berney et al. demonstrated that blocking methionine biosynthesis in *M. tuberculosis* rendered this pathogen exquisitely sensitive to death in mice (38). Thus, the methionine biosynthesis pathway seems to be an attractive target for designing new anti-TB drugs, especially given the global crisis of drug-resistant *M. tuberculosis*.

As a key enzyme responsible for producing a crucial cofactor required for methionine biosynthesis in *M. tuberculosis*, Rv2172c itself seems to be a good target for designing new anti-TB drugs. It is essential for the *in vitro* growth of *M. tuberculosis* and might also be important for the survival of this bacterium in a host, which merits further investigation. The fact that decreasing the activity of Rv2172c makes *M. tuberculosis* more sensitive to PAS and SMX implies that inhibitors of this protein can be used in combinations with other existing drugs. Although humans also have an MTHFR (39), considerable structural differences have been observed between it and Rv2172c (see Fig. S3 in the supplemental material).

Due to its essentiality for bacterial growth, the mutation rate of *rv2172c* is rather low (1.49%) in clinical isolates. However, missense mutations could be identified in 9.62% (5/52) of PAS-resistant clinical isolates, and one specific mutation, T120P, could be identified in 5.77% (3/52) of PAS-resistant clinical isolates but not in PAS-sensitive isolates. These data indicate a potential clinical relevance of *rv2172c* and PAS suscepti-

TABLE 2 Methionine reverts the sensitivity of Rv2172c L214A and R159N to PAS in *M. tuberculosis* H37Ra

	MIC (μg $\cdot$ mL^{-1}) for:	
Strain[a]	PAS	PAS added with 150 μM Met
Rv2172c (WT)	0.2	1.6
Rv2172c (L214A)	0.01	0.4
Rv2172c (R159N)	0.01	0.4

[a]Rv2172c (WT), H37Ra Δ*rv2172c* pMV361::*rv2172c*. Rv2172c (L214A), H37Ra Δ*rv2172c* pMV361::*rv2172c* (L214A). Rv2172c (R159N), H37Ra Δ*rv2172c* pMV361::*rv2172c* (R159N).

TABLE 3 Overexpression of primary genes that participate in methionine biosynthesis confers PAS resistance in *M. tuberculosis* H37Ra

Strain[a]	MIC ($\mu g \cdot mL^{-1}$) of PAS
WT	0.02
MetE+	0.1
MetH+	0.1
rv2172c+	0.2

[a]WT, H37Ra pMV261. *MetE*+, H37Ra pMV261::*metE*. *MetH*+, H37Ra pMV261::*metH*. *rv2172c*+, H37Ra pMV261:: *rv2172c*.

bility, which merits further investigation.

In summary, we identified Rv2172c as an MTHFR in *M. tuberculosis* and revealed that Arg159 and Leu214 are key catalytic residues for its MTHFR activity. As a result, mutation of the above two residues in Rv2172c caused decreased production of methionine in *M. tuberculosis* and increased susceptibility to PAS. As expected, *rv2172c* was shown to be essential for the *in vitro* growth of *M. tuberculosis*, but this essentiality was not limited to methionine biosynthesis. Our data, in combination with previous studies, indicate that Rv2172c might be a good target for designing new anti-TB drugs.

MATERIALS AND METHODS

Bacterial strains, plasmids, and culture conditions. *M. tuberculosis* H37Ra and derivative strains were cultured at 37°C in 7H9 broth (Difco) supplemented with 10% (vol/vol) oleic acid-albumin-dextrose-catalase (OADC; Difco), 0.5% (vol/vol) glycerol, and 0.05% (vol/vol) Tween 80 (Sigma-Aldrich), or on 7H10 agar medium (Difco) supplemented with 10% (vol/vol) OADC (Difco) and 0.5% (vol/vol) glycerol. *M. smegmatis* mc²155 was grown in Middlebrook 7H9 medium or 7H10 agar medium. *E. coli* W3110 and derivative strains were cultured in medium E supplemented with 0.5% (vol/vol) dextrose, Luria-Bertani (LB) medium (Difco), or on LB agar plates at 37°C. All bacterial strains, plasmids, and primers used in this study are described in detail in Table S1 in the supplemental material.

Antibiotics and chemicals. In total, of 75 $\mu g \cdot mL^{-1}$ and 150 $\mu g \cdot mL^{-1}$ hygromycin (Sigma-Aldrich), 25 $\mu g \cdot mL^{-1}$ and 100 $\mu g \cdot mL^{-1}$ kanamycin (MD Bio, Inc.), 150 $\mu g \cdot mL^{-1}$ ampicillin (MD Bio, Inc.), 50 $\mu g \cdot mL^{-1}$ chloramphenicol (MD Bio, Inc.), and 3.75 to 300 μM methionine (Sigma) were used, unless otherwise indicated. 5,10-Methylenetetrahydrofolate and 5-methyltetrahydrofolate were purchased from Schircks Laboratories. PAS and SMX (Sigma) were used at indicated concentrations.

3D structure modeling. Structural modeling of Rv2172c (UniProtKB accession number O53506) was carried out with the assistance of SWISS-MODEL (40, 41). After searching in the database (https:// swissmodel.expasy.org), a suitable template was selected. The structure of the target protein was modeled based on a template in PyMOL, and then graphs were exported for visualization.

Construction of *E. coli* and *M. tuberculosis* mutants and complementary strains. An unmarked deletion strain of *metF* was constructed as previously described (42). The introduced kanamycin-resistant cassettes were eliminated by transformation with plasmid pCP20. For the construction of complementation strains, genomic DNA from *E. coli* and *M. tuberculosis* was extracted. Fragments of *metF* and *rv2172c* were amplified by PCR using specific primers, then ligated into plasmid pCA24N to obtain pCA24N::*metF* and pCA24N::*rv2172c*, respectively. A modified strategy for phage-mediated allelic exchange (43) was used to construct *M. tuberculosis* H37Ra derivatives containing the derived alleles R159N and L214A. Briefly, *rv2172c* (wild-type) and *rv2172c* alleles were cloned into pMV361 and used to transform *M. tuberculosis* H37Ra. The native copy of *rv2172c* was deleted by specialized transduction using phAE159 containing a hygromycin resistance cassette. All primers used are listed in Table S1.

Growth curves. *E. coli* W3110 strains and *M. tuberculosis* strains were cultured to the log phase in medium E containing 0.5% (vol/vol) glucose and separately in 7H9 broth containing OADC at 37°C, then diluted by 10-fold serial dilutions to about 10^6 CFU $\cdot$ mL^{-1} and 10^5 CFU $\cdot$ mL^{-1}, respectively, in 10 mL fresh medium E with 0.5% glucose and separately in 7H9 broth containing OADC. Then, bacteria were incubated at 37°C. The growth of bacterial cultures was measured by monitoring the optical density at 600 nm (OD$_{600}$) using a spectrophotometer at specified time points (Bio-Rad). Where appropriate, culture

TABLE 4 Mutation rates of *rv2172c* among 6,568 *M. tuberculosis* genomes

Mutation type	Rate (%) in:	
	Clinic	Environment
All types	1.49	8.14
Synonymous SNP	0.16	5.04
Nonsynonymous SNP	1.08	1.16
Indel or nonsense SNP	0.03	0.00

TABLE 5 Gene mutation analysis in 52 PAS-resistant *M. tuberculosis* clinical isolates

Gene	Mutation type	Count	
		No.	%
folC		21	40.38
	E40G	9	17.31
	S150G	6	11.54
	I43T	2	3.85
	E153A	1	1.92
	E153G	1	1.92
	S98G	1	1.92
	A420V	1	1.92
thyA		18	34.62
	T202A	12	23.08
	S215F	1	1.92
	T26P	1	1.92
	H75N	1	1.92
	thyA-dfrA deletion	2	3.85
	thyA deletion	1	1.92
rv2172c		5	9.62
	T120P	3	5.77
	M172V	2	3.85
ribD		2	3.85
	$^{-11}$G>A	2	3.85

medium was supplemented with corresponding levels of methionine. At each time point, a sample of each culture was taken, and serial dilutions were plated on Middlebrook 7H10 plates (for *M. tuberculosis*) or LB agar plates (for *E. coli*). The plates were incubated in a normal aerobic atmosphere at 37°C for 2 to 3 weeks (*M. tuberculosis*) or overnight (*E. coli*), and the CFU were counted as in a previous study (44). The graphs for growth analysis were prepared using Origin, and the mean values with standard deviations (SDs) were plotted against time.

Protein purification. Rv2172c was purified as previously reported (33), with some changes. Briefly, *rv2172c* was amplified from *M. tuberculosis* H37Ra genomic DNA using specific primers (Table S1) and was cloned into pMAL-c2XHis2 to yield pMAL-c2XHis2::*rv2172c*, which introduced an N-terminal maltose-binding protein (MBP) tag linked with a factor Xa cleavage site and a C-terminal histidine tag. After sequence verification, the recombinant plasmid was transformed into *E. coli* BL21(DE3). The cells were grown at 37°C in LB broth to an OD_{600} of ~0.6, isopropyl-β-D-thiogalactopyranoside (IPTG; Acmec) was added to 0.25 mM, and the cells were incubated further at 16°C for 20 h. The bacterial cells were harvested by centrifugation, resuspended in column buffer (CB; 50 mM Tris-HCl and 500 mM NaCl [pH 8.0]) and then disrupted by sonication. Recombinant Rv2172c proteins were first purified over an amylose resin column (product no. E8021; New England Biolabs). To remove the MBP tag, the purified samples were incubated with factor Xa at 4°C overnight in reaction buffer (20 mM HEPES [pH 8.0], 100 mM NaCl, 2 mM $CaCl_2$, and 10% glycerol). These cleavage samples were then loaded on prewashed nickel-nitrilotriacetic acid HisTrap HP affinity resin (GE Healthcare) at 4°C overnight, and nonspecifically bound protein was removed by washing this resin with 50 mM Tris-HCl, 500 mM NaCl, and 60 mM imidazole (pH 8.0), while recombinant Rv2172c was eluted with 50 mM Tris-HCl, 500 M NaCl, and 200 mM imidazole (pH 8.0). The fractions were then analyzed by SDS-PAGE.

***In vitro* enzymatic activity assays.** The MTHFR activity of Rv2172c was measured by HPLC-MS. Five reaction systems (500 μL) were designed to assay purified Rv2172c for its reductase activity *in vitro*. Reaction system 1 contained 100 mM NaH_2PO_4, 100 mM Na_2HPO_4 (pH 8.0), 2 mM NADH, 100 μM FAD, and 10 mM 5,10-CH_2-THF. Reaction system 2 contained 100 mM NaH_2PO_4, 100 mM Na_2HPO_4 (pH 8.0), 10 μM Rv2172c, 2 mM NADH, 100 μM FAD, and 10 mM 5,10-CH_2-THF. Reaction system 3 contained 100 mM NaH_2PO_4, 100 mM Na_2HPO_4 (pH 8.0), 10 μM Rv2172c, 100 μM FAD, and 10 mM 5,10-CH_2-THF. Reaction system 4 contained 100 mM NaH_2PO_4, 100 mM Na_2HPO_4 (pH 8.0), 10 μM Rv2172c, 2 mM NADH, and 10 mM 5,10-CH_2-THF. Reaction system 5 contained 100 mM NaH_2PO_4, 100 mM Na_2HPO_4 (pH 8.0), 10 μM Rv2172c, 2 mM NADH, and 100 μM FAD. All reaction mixtures were incubated at 37°C for 2 h in triplicate, then centrifuged over Microcon-10 protein filter columns at 4°C and 1,000 rpm for 20 min to remove Rv2172c protein. The reaction mixtures were then injected onto a Phenomenex Luna 3-μm C_{18} 100-Å liquid chromatography (LC) column (50 mm × 2 mm) on an UltiMate 3000 ultraperformance liquid chromatography (UPLC) system (Thermo Fisher Scientific). Samples were eluted with a gradient from 90% buffer A (methanol plus 0.1% formic acid) and 10% buffer B (H_2O plus 0.1% formic acid) to 100% buffer B for 30 min, from 100% buffer B to 100% buffer B for 5 min, and from 100% buffer B to 5% buffer B for 1 min, at a flow rate of 0.3 mL/min. The peaks of the substrate, 5,10-CH_2-THF, and the product, 5-CH_3-THF, were measured by UV absorbance (A_{254}) and confirmed by electrospray ionization-mass spectrometry (ESI-MS) using an in-line LCQ Fleet ion trap mass spectrometer (Thermo Fisher Scientific). The ESI-MS working parameters were as follows: 4.5 kV capillary voltage, 300°C heat block temperature

for analysis, and nitrogen drying and nebulizer gases set at 1.5 L/min. The HPLC-MS data were acquired in a scan range between 100 and 1,000 m/z using the negative ionization mode.

Drug susceptibility testing. Mycobacterial cells were cultured to the mid-log phase (OD_{600} = 0.5 to 1.0) and diluted to about 10^5 CFU · mL^{-1} using 10-fold serial dilutions in fresh 7H9 medium with or without 10% OADC. Then, bacterial cells were plated on 7H10 solid agar plates containing the following drugs at different concentrations: PAS (0, 0.002, 0.005, 0.01, 0.02, 0.05, 0.1, 0.2, 0.4, 0.8, 1.6, 3.2, and 6.4 μg · mL^{-1}) or SMX (0, 0.78125, 1.5625, 3.125, 6.25, 12.5, 25, 50, 100, and 200 μg · mL^{-1}). Where appropriate, culture medium was supplemented with 150 μM methionine. All antibiotics were purchased from Sigma-Aldrich and solubilized according to the manufacturer's recommendations. Cultures were then incubated at 37°C for 21 days. The MIC was defined as the lowest concentration of antibiotics required to inhibit 99% of CFUs after this culture period. The MICs were performed through two technical repetitions using three biological replicates. All of the bacterial strains used are listed in Table S1.

Antibiotic killing assays. Bacteria were grown to an OD_{600} of 0.5 to 1.0, diluted to an OD_{600} of ~0.1 (10^7 CFU · mL^{-1}) in fresh 7H9 medium with OADC, and treated with 2.5 μg · mL^{-1} PAS. Cultures were incubated at 37°C, and aliquots of samples were separately plated on 7H10 medium after serial dilution at days 0, 2, 5, 7, 14, and 21. Where appropriate, culture medium was supplemented with corresponding methionine. Graphs for antibiotic kill curves were prepared using Origin, and the mean values with standard deviations (SDs) were plotted against time.

Determination of methionine content *in vivo*. Quantitative detection of L-methionine by UPLC-MS/MS was done using an optimized method previously reported (45). Bacterial samples (~10^9 CFU) were resuspended in 0.4 mL precooled methanol-water (2:1, vol/vol) and subjected to three freeze-thaw cycles before sonication in an ice bath for 15 min (cycles: 1-min pulse followed by 1-min pause). The above-described extraction procedure was repeated twice. The mixture was then centrifuged for 10 min at 12,000 × g at 4°C, and 10 μL of each supernatant was mixed with 87.5 μL borate buffer (0.2 M, pH 8.8) containing 20 mM Tris(2-carboxyethyl)phosphine hydrochloride (TCEP) and 5 mM ascorbic acid. After vortex mixing and incubation at room temperature for 1 min, the samples were mixed with 33 μL 5-aminoisoquinolyl-*N*-hydroxysuccinimidyl carbamate (5-AIQC) solution and incubated at 55°C for 10 min. The mixture was then cooled down to ambient temperature, and 2 μL of formic acid was added. The mixture was centrifuged for 10 min at 12,000 × g at 4°C, and 10 μL of each supernatant was filtered using a 0.22-μm membrane filter before UPLC-MS/MS analysis. UPLC-MS/MS was performed using an Agilent 1290 UPLC instrument coupled to an Agilent 6470 triple quadrupole mass spectrometer equipped with an electrospray ionization (ESI) source (Agilent Technologies, USA). The 5-AIQC-tagged samples (1 μL) were individually injected on an UPLC column (Agilent Zorbax RRHD Eclipse XDB C_{18} column, 2.1 mm × 50 mm, 1.8-μm particles) with the temperature set to 50°C. Water containing 2 mM ammonium bicarbonate and methanol containing 0.16% (vol/vol) formic acid and ammonium formate were used as the two mobile phases A and B, respectively, with a flow rate of 0.5 mL/min. An optimized gradient elution scheme was employed as 5 to 16% B (0 to 2.5 min), 16 to 22.5% B (2.5 to 6 min), 22.5 to 95% B (6 to 8.5 min), and 95% B (8.5 to 12 min). Electrospray ionization was performed using the positive ion mode, the pressure of the nebulizer was 50 lb/in², the sheath gas temperature was 350°C with a flow rate of 10 L/min, the dry gas temperature was 315°C with a flow rate of 10 L/min, and the capillary was set at 4,000 V. Multiple reaction monitoring (MRM) was used for the quantification of screening fragment ions. Peak determination and peak area integration were performed using Mass Hunter Workstation software (version B.08.00; Agilent). Standard curves were constructed by least-squares linear regression analysis using the peak area ratio of derivatized individual standards against the nominal concentration of the calibrator. The quantification of samples was performed identically. The bacterial biomasses of the individual samples were determined by measuring the residual protein content of the metabolite extracts (6). All data obtained by metabolomics were average of independent sextuplicates. P values were calculated using t tests. The graphs for the determination of methionine *in vivo* were prepared using GraphPad Prism, and median values with 95% confidence levels (CL) were plotted.

Library preparation and whole-genome sequencing. Eight individual clinical isolates were provided and characterized as PAS resistant via drug susceptibility testing (DST) by Chongqing Public Health Medical Center (46). Library preparation and whole-genome sequencing were performed at Shanghai Biotechnology Corporation, People's Republic of China. Genomic DNA of the 8 isolates was extracted from freshly cultured bacteria using the HiPure mycobacteria DNA kit (Magen, Guangzhou, China) following the manufacturer's protocol. A library was prepared using the NEBNext Ultra DNA library prep kit for Illumina (NEB, USA) following the manufacturer's protocol and sequenced on a HiSeq 2500 system (Illumina, USA). Library concentration was detected using a Qubit 2.0 fluorometer (Invitrogen, USA) and the Qubit double-stranded DNA (dsDNA) high-sensitivity (HS) kit (Invitrogen, USA). The size and purity of the library were detected using the 2100 Bioanalyzer (Agilent, USA). Raw sequence data were mapped to *M. tuberculosis* H37Rv reference genome (GenBank accession number AL123456.3) using Bowtie 2 version 2-2.0.5. Single-nucleotide polymorphisms (SNPs) and indels were detected using SAMtools version 1.14 (47).

Comparative analysis of variants in *M. tuberculosis* genomes. As shown in Table S2, a library of *M. tuberculosis* genomes with the classifications "clinical" (n = 6,310) or "environmental" (n = 258) was downloaded from the NCBI database. In addition, the genomes of 8 PAS-resistant clinical isolates we recently obtained and genomes of other PAS0resistant or PAS0sensitive clinical isolates (n = 44 and 66, respectively) presented in previous research (48–54) are listed in Table S3. All of the raw reads were available and selected after quality inspection. The reference *rv2172c*, *folC*, *thyA*, and *ribD* genes were determined using *M. tuberculosis* H37Rv (GenBank accession no. NC_000962.3). The homologous genes from other isolates were identified based on the corresponding reference gene using the Basic Local

Alignment Search Tool (BLAST) with the default options chosen. All sequences were aligned to the targeted gene fragments using Geneious (v10.2.6). The variation positions were extracted and analyzed using an in-house script.

Data availability. All reads generated in this study were deposited in the Sequence Read Archive under accession no. PRJNA774929.

SUPPLEMENTAL MATERIAL

Supplemental material is available online only.
SUPPLEMENTAL FILE 1, PDF file, 0.7 MB.
SUPPLEMENTAL FILE 2, XLSX file, 0.5 MB.
SUPPLEMENTAL FILE 3, XLSX file, 0.01 MB.

REFERENCES

1. World Health Organization. 2020. Global tuberculosis report 2019. World Health Organization, Geneva, Switzerland.
2. Cobbold RJ, Morrison GD, Willcox RR. 1968. Treatment of gonorrhoea with single oral doses of rifampicin. Br Med J 4:681–682. https://doi.org/10.1136/bmj.4.5632.681.
3. Gandhi NR, Moll A, Sturm AW, Pawinski R, Govender T, Lalloo U, Zeller K, Andrews J, Friedland G. 2006. Extensively drug-resistant tuberculosis as a cause of death in patients co-infected with tuberculosis and HIV in a rural area of South Africa. Lancet 368:1575–1580. https://doi.org/10.1016/S0140-6736(06)69573-1.
4. Pitchenik AE, Burr J, Laufer M, Miller G, Cacciatore R, Bigler WJ, Witte JJ, Cleary T. 1990. Outbreaks of drug-resistant tuberculosis at AIDS centre. Lancet 336:440–441. https://doi.org/10.1016/0140-6736(90)91987-l.
5. Lehmann J. 1946. *Para*-aminosalicylic acid in the treatment of tuberculosis. Lancet 1:15. https://doi.org/10.1016/S0140-6736(46)91185-3.
6. Chakraborty S, Gruber T, Barry CE, 3rd, Boshoff HI, Rhee KY. 2013. *Para*-aminosalicylic acid acts as an alternative substrate of folate metabolism in *Mycobacterium tuberculosis*. Science 339:88–91. https://doi.org/10.1126/science.1228980.
7. Zheng J, Rubin EJ, Bifani P, Mathys V, Lim V, Au M, Jang J, Nam J, Dick T, Walker JR, Pethe K, Camacho LR. 2013. *Para*-aminosalicylic acid is a prodrug targeting dihydrofolate reductase in *Mycobacterium tuberculosis*. J Biol Chem 288:23447–23456. https://doi.org/10.1074/jbc.M113.475798.
8. Thijssen HH. 1973. The formation of H$_2$-pteroate analogs from PABA-antagonists in a cell-free system of *E. coli*. Arch Int Pharmacodyn Ther 206:272–281.
9. Hitchings GH. 1973. Mechanism of action of trimethoprim-sulfamethoxazole—I. J Infect Dis 128:433–436.
10. Thijssen HH. 1974. Relation between structure of sulphonamides and inhibition of H2-pteroate synthesis in *Escherichia coli*. J Pharm Pharmacol 26:228–234. https://doi.org/10.1111/j.2042-7158.1974.tb09263.x.
11. Patole J, Shingnapurkar D, Padhye S, Ratledge C. 2006. Schiff base conjugates of *p*-aminosalicylic acid as antimycobacterial agents. Bioorg Med Chem Lett 16:1514–1517. https://doi.org/10.1016/j.bmcl.2005.12.035.
12. Zumla A, Nahid P, Cole ST. 2013. Advances in the development of new tuberculosis drugs and treatment regimens. Nat Rev Drug Discov 12:388–404. https://doi.org/10.1038/nrd4001.
13. Alsaad N, Dijkstra JA, Akkerman OW, de Lange WC, van Soolingen D, Kosterink JG, van der Werf TS, Alffenaar JW. 2016. Pharmacokinetic evaluation of sulfamethoxazole at 800 milligrams once daily in the treatment of tuberculosis. Antimicrob Agents Chemother 60:3942–3947. https://doi.org/10.1128/AAC.02175-15.
14. Cavanaugh JS, Jou R, Wu MH, Dalton T, Kurbatova E, Ershova J, Cegielski JP, Global PI, Global PETTS Investigators. 2017. Susceptibilities of MDR *Mycobacterium tuberculosis* isolates to unconventional drugs compared with their reported pharmacokinetic/pharmacodynamic parameters. J Antimicrob Chemother 72:1678–1687. https://doi.org/10.1093/jac/dkx022.
15. Palomino JC, Martin A. 2016. The potential role of trimethoprim-sulfamethoxazole in the treatment of drug-resistant tuberculosis. Future Microbiol 11:539–547. https://doi.org/10.2217/fmb.16.2.
16. Green JM, Matthews RG. 2007. Folate biosynthesis, reduction, and polyglutamylation and the interconversion of folate derivatives. EcoSal Plus 2. https://doi.org/10.1128/ecosalplus.3.6.3.6.
17. Hedgecock LW. 1956. Antagonism of the inhibitory action of aminosalicylic acid on *Mycobacterium tuberculosis* by methionine, biotin and certain fatty acids, amino acids, and purines. J Bacteriol 72:839–846. https://doi.org/10.1128/jb.72.6.839-846.1956.
18. Hedgecock LW. 1958. Antagonism of methionine in aminosalicylate-inhibition of *Mycobacterium tuberculosis*. J Bacteriol 75:417–421. https://doi.org/10.1128/jb.75.4.417-421.1958.
19. Sheppard CA, Trimmer EE, Matthews RG. 1999. Purification and properties of NADH-dependent 5,10-methylenetetrahydrofolate reductase (MetF) from E*scherichia coli*. J Bacteriol 181:718–725. https://doi.org/10.1128/JB.181.3.718-725.1999.
20. Matthews RG, Sheppard C, Goulding C. 1998. Methylenetetrahydrofolate reductase and methionine synthase: biochemistry and molecular biology. Eur J Pediatr 157:S54–S59. https://doi.org/10.1007/pl00014305.
21. Vanoni MA, Ballou DP, Matthews RG. 1983. Methylenetetrahydrofolate reductase: steady state and rapid reaction studies on the NADPH-methylenetetrahydrofolate, NADPH-menadione, and methyltetrahydrofolate-menadione oxidoreductase activities of the enzyme. J Biol Chem 258:11510–11514. https://doi.org/10.1016/S0021-9258(17)44257-8.
22. Bertsch J, Oppinger C, Hess V, Langer JD, Muller V. 2015. Heterotrimeric NADH-oxidizing methylenetetrahydrofolate reductase from the acetogenic bacterium *Acetobacterium woodii*. J Bacteriol 197:1681–1689. https://doi.org/10.1128/JB.00048-15.
23. Guenther BD, Sheppard CA, Tran P, Rozen R, Matthews RG, Ludwig ML. 1999. The structure and properties of methylenetetrahydrofolate reductase from *Escherichia coli* suggest how folate ameliorates human hyperhomocysteinemia. Nat Struct Biol 6:359–365. https://doi.org/10.1038/7594.
24. Pejchal R, Campbell E, Guenther BD, Lennon BW, Matthews RG, Ludwig ML. 2006. Structural perturbations in the Ala → Val polymorphism of methylenetetrahydrofolate reductase: how binding of folates may protect against inactivation. Biochemistry 45:4808–4818. https://doi.org/10.1021/bi052294c.

25. Trimmer EE, Ballou DP, Ludwig ML, Matthews RG. 2001. Folate activation and catalysis in methylenetetrahydrofolate reductase from *Escherichia coli*: roles for aspartate 120 and glutamate 28. Biochemistry 40:6216–6226. https://doi.org/10.1021/bi002790v.

26. Pejchal R, Sargeant R, Ludwig ML. 2005. Structures of NADH and CH$_3$-H$_4$folate complexes of *Escherichia coli* methylenetetrahydrofolate reductase reveal a spartan strategy for a ping-pong reaction. Biochemistry 44:11447–11457. https://doi.org/10.1021/bi050533q.

27. Lee MN, Takawira D, Nikolova AP, Ballou DP, Furtado VC, Phung NL, Still BR, Thorstad MK, Tanner JJ, Trimmer EE. 2009. Functional role for the conformationally mobile phenylalanine 223 in the reaction of methylenetetrahydrofolate reductase from *Escherichia coli*. Biochemistry 48:7673–7685. https://doi.org/10.1021/bi9007325.

28. Young DB, Comas I, de Carvalho LP. 2015. Phylogenetic analysis of vitamin B12-related metabolism in *Mycobacterium tuberculosis*. Front Mol Biosci 2:6. https://doi.org/10.3389/fmolb.2015.00006.

29. Kelley LA, Mezulis S, Yates CM, Wass MN, Sternberg MJ. 2015. The Phyre2 web portal for protein modeling, prediction and analysis. Nat Protoc 10:845–858. https://doi.org/10.1038/nprot.2015.053.

30. Gonzalez JC, Banerjee RV, Huang S, Sumner JS, Matthews RG. 1992. Comparison of cobalamin-independent and cobalamin-dependent methionine synthases from *Escherichia coli*: two solutions to the same chemical problem. Biochemistry 31:6045–6056. https://doi.org/10.1021/bi00141a013.

31. Sah S, Lahry K, Talwar C, Singh S, Varshney U. 2020. Monomeric NADH-oxidizing methylenetetrahydrofolate reductases from *Mycobacterium smegmatis* lack flavin coenzyme. J Bacteriol 202:e00709-19. https://doi.org/10.1128/JB.00709-19.

32. Zhang X, Liu L, Zhang Y, Dai G, Huang H, Jin Q. 2015. Genetic determinants involved in *p*-aminosalicylic acid resistance in clinical isolates from tuberculosis patients in northern China from 2006 to 2012. Antimicrob Agents Chemother 59:1320–1324. https://doi.org/10.1128/AAC.03695-14.

33. Zhao F, Wang XD, Erber LN, Luo M, Guo AZ, Yang SS, Gu J, Turman BJ, Gao YR, Li DF, Cui ZQ, Zhang ZP, Bi LJ, Baughn AD, Zhang XE, Deng JY. 2014. Binding pocket alterations in dihydrofolate synthase confer resistance to *para*-aminosalicylic acid in clinical isolates of *Mycobacterium tuberculosis*. Antimicrob Agents Chemother 58:1479–1487. https://doi.org/10.1128/AAC.01775-13.

34. Mathys V, Wintjens R, Lefevre P, Bertout J, Singhal A, Kiass M, Kurepina N, Wang XM, Mathema B, Baulard A, Kreiswirth BN, Bifani P. 2009. Molecular genetics of *para*-aminosalicylic acid resistance in clinical isolates and spontaneous mutants of *Mycobacterium tuberculosis*. Antimicrob Agents Chemother 53:2100–2109. https://doi.org/10.1128/AAC.01197-08.

35. Rengarajan J, Sassetti CM, Naroditskaya V, Sloutsky A, Bloom BR, Rubin EJ. 2004. The folate pathway is a target for resistance to the drug para-aminosalicylic acid (PAS) in mycobacteria. Mol Microbiol 53:275–282. https://doi.org/10.1111/j.1365-2958.2004.04120.x.

36. Howe MD, Kordus SL, Cole MS, Bauman AA, Aldrich CC, Baughn AD, Minato Y. 2018. Methionine antagonizes *para*-aminosalicylic acid activity via affecting folate precursor biosynthesis in *Mycobacterium tuberculosis*. Front Cell Infect Microbiol 8:399. https://doi.org/10.3389/fcimb.2018.00399.

37. Guzzo MB, Nguyen HT, Pham TH, Wyszczelska-Rokiel M, Jakubowski H, Wolff KA, Ogwang S, Timpona JL, Gogula S, Jacobs MR, Ruetz M, Krautler B, Jacobsen DW, Zhang GF, Nguyen L. 2016. Methylfolate trap promotes bacterial thymineless death by sulfa drugs. PLoS Pathog 12:e1005949. https://doi.org/10.1371/journal.ppat.1005949.

38. Berney M, Berney-Meyer L, Wong KW, Chen B, Chen M, Kim J, Wang J, Harris D, Parkhill J, Chan J, Wang F, Jacobs WR, Jr. 2015. Essential roles of methionine and *S*-adenosylmethionine in the autarkic lifestyle of *Mycobacterium tuberculosis*. Proc Natl Acad Sci U S A 112:10008–10013. https://doi.org/10.1073/pnas.1513033112.

39. Froese DS, Kopec J, Rembeza E, Bezerra GA, Oberholzer AE, Suormala T, Lutz S, Chalk R, Borkowska O, Baumgartner MR, Yue WW. 2018. Structural basis for the regulation of human 5,10-methylenetetrahydrofolate reductase by phosphorylation and *S*-adenosylmethionine inhibition. Nat Commun 9:2261. https://doi.org/10.1038/s41467-018-04735-2.

40. Arnold K, Bordoli L, Kopp J, Schwede T. 2006. The SWISS-MODEL workspace: a web-based environment for protein structure homology modelling. Bioinformatics 22:195–201. https://doi.org/10.1093/bioinformatics/bti770.

41. Biasini M, Bienert S, Waterhouse A, Arnold K, Studer G, Schmidt T, Kiefer F, Gallo Cassarino T, Bertoni M, Bordoli L, Schwede T. 2014. SWISS-MODEL: modelling protein tertiary and quaternary structure using evolutionary information. Nucleic Acids Res 42:W252–258. https://doi.org/10.1093/nar/gku340.

42. Datsenko KA, Wanner BL. 2000. One-step inactivation of chromosomal genes in *Escherichia coli* K-12 using PCR products. Proc Natl Acad Sci U S A 97:6640–6645. https://doi.org/10.1073/pnas.120163297.

43. Bardarov S, Bardarov S, Pavelka MS, Sambandamurthy V, Larsen M, Tufariello J, Chan J, Hatfull G, Jacobs WR. 2002. Specialized transduction: an efficient method for generating marked and unmarked targeted gene disruptions in *Mycobacterium tuberculosis*, *M. bovis* BCG and *M. smegmatis*. Microbiology (Reading) 148:3007–3017. https://doi.org/10.1099/00221287-148-10-3007.

44. Vilcheze C, Jacobs WR, Jr. 2012. The combination of sulfamethoxazole, trimethoprim, and isoniazid or rifampin is bactericidal and prevents the emergence of drug resistance in *Mycobacterium tuberculosis*. Antimicrob Agents Chemother 56:5142–5148. https://doi.org/10.1128/AAC.00832-12.

45. Wang J, Zhou L, Lei H, Hao F, Liu X, Wang Y, Tang H. 2017. Simultaneous quantification of amino metabolites in multiple metabolic pathways using ultra-high performance liquid chromatography with tandem-mass spectrometry. Sci Rep 7:1423. https://doi.org/10.1038/s41598-017-01435-7.

46. Luo M, Li K, Zhang H, Yan X, Gu J, Zhang Z, Chen Y, Li J, Wang J, Chen Y. 2019. Molecular characterization of *para*-aminosalicylic acid resistant *Mycobacterium tuberculosis* clinical isolates in southwestern China. Infect Drug Resist 12:2269–2275. https://doi.org/10.2147/IDR.S207259.

47. Li H, Handsaker B, Wysoker A, Fennell T, Ruan J, Homer N, Marth G, Abecasis G, Durbin R, Genome Project Data Processing Subgroup. 2009. The Sequence Alignment/Map format and SAMtools. Bioinformatics 25:2078–2079. https://doi.org/10.1093/bioinformatics/btp352.

48. Brown AC, Bryant JM, Einer-Jensen K, Holdstock J, Houniet DT, Chan JZ, Depledge DP, Nikolayevskyy V, Broda A, Stone MJ, Christiansen MT, Williams R, McAndrew MB, Tutill H, Brown J, Melzer M, Rosmarin C, McHugh TD, Shorten RJ, Drobniewski F, Speight G, Breuer J. 2015. Rapid whole-genome sequencing of *Mycobacterium tuberculosis* isolates directly from clinical samples. J Clin Microbiol 53:2230–2237. https://doi.org/10.1128/JCM.00486-15.

49. Witney AA, Gould KA, Arnold A, Coleman D, Delgado R, Dhillon J, Pond MJ, Pope CF, Planche TD, Stoker NG, Cosgrove CA, Butcher PD, Harrison TS, Hinds J. 2015. Clinical application of whole-genome sequencing to inform treatment for multidrug-resistant tuberculosis cases. J Clin Microbiol 53:1473–1483. https://doi.org/10.1128/JCM.02993-14.

50. Phelan J, O'Sullivan DM, Machado D, Ramos J, Whale AS, O'Grady J, Dheda K, Campino S, McNerney R, Viveiros M, Huggett JF, Clark TG. 2016. The variability and reproducibility of whole genome sequencing technology for detecting resistance to anti-tuberculous drugs. Genome Med 8:132. https://doi.org/10.1186/s13073-016-0385-x.

51. Doyle RM, Burgess C, Williams R, Gorton R, Booth H, Brown J, Bryant JM, Chan J, Creer D, Holdstock J, Kunst H, Lozewicz S, Platt G, Romero EY, Speight G, Tiberi S, Abubakar I, Lipman M, McHugh TD, Breuer J. 2018. Direct whole-genome sequencing of sputum accurately identifies drug-resistant *Mycobacterium tuberculosis* faster than MGIT culture sequencing. J Clin Microbiol 56:e00666-18. https://doi.org/10.1128/JCM.00666-18.

52. Li H, Kayani M, Gu Y, Wang X, Zhu T, Duan H, Ma Y, Huang H, Javid B. 2015. Transmitted extended-spectrum extensively drug-resistant tuberculosis in Beijing, China, with discordant whole-genome sequencing analysis results. J Clin Microbiol 53:2781–2784. https://doi.org/10.1128/JCM.00891-15.

53. Nonghanphithak D, Kaewprasert O, Chaiyachat P, Reechaipichitkul W, Chaiprasert A, Faksri K. 2020. Whole-genome sequence analysis and comparisons between drug-resistance mutations and minimum inhibitory concentrations of *Mycobacterium tuberculosis* isolates causing M/XDR-TB. PLoS One 15:e0244829. https://doi.org/10.1371/journal.pone.0244829.

54. Fernandez Do Porto DA, Monteserin J, Campos J, Sosa EJ, Matteo M, Serral F, Yokobori N, Benevento AF, Poklepovich T, Pardo A, Wainmayer I, Simboli N, Castello F, Paul R, Marti M, Lopez B, Turjanski A, Ritacco V. 2021. Five-year microevolution of a multidrug-resistant *Mycobacterium tuberculosis* strain within a patient with inadequate compliance to treatment. BMC Infect Dis 21:394. https://doi.org/10.1186/s12879-021-06069-9.